

PMF, Cesium & Rubidium Nanoparticles Induce Apoptosis in A549 Cells

Faten. A. Khorshid¹; Gehan. A. Raouf² *; Salem. M. El-Hamidy³; Gehan. S. Al-amri¹; Nourah. A. Alotaibi² and Taha A. Kumosani²

King Fahd Medical Research Centre, ¹Tissue Culture Unit, ²Medical Biophysics Laboratory, Biochemistry Department, ³ Electron Microscopy Unit, Biological Science Department and ²Biochemistry Department, Faculty of Science, King Abdulaziz University
*jahmed@kau.edu.sa

Abstract: Cancer becomes one of the leading cause of death in many countries over the world. Fourier-transform infrared (FTIR) spectra of human lung cancer cells (A549) treated with PMF (natural product extracted from PM 701) for different time intervals were examined. Second derivative and difference method were taken in comparison studies. Cesium (Cs) and Rubidium (Rb) nanoparticles in PMF were detected by Energy Dispersive X-ray attached to Scanning Electron Microscope SEM-EDX. Characteristic changes in protein secondary structure, lipid profile and changes in the intensities of DNA bands were identified in treated A549 cells spectra. A characteristic internucleosomal ladder of DNA fragmentation was also observed after 30 min of treatment. Moreover, the pH values were significantly increases upon treatment due to the presence of Cs and Rb nanoparticles in the PMF fraction. These results support the previous findings that PMF is selective anticancer agent and can produce apoptosis to A549 cells.

[Faten. A. Khorshid; Gehan. A. Raouf; Salem. M. El-Hamidy; Gehan. S. Al-amri¹; Nourah. A. Alotaibi and Taha A. Kumosani, PMF, Cesium & Rubidium Nanoparticles Induce Apoptosis in A549 Cells] Life Science Journal, 2011; 8(3):534-542] (ISSN: 1097-8135). <http://www.lifesciencesite.com>.

Keywords: Apoptosis, FTIR spectroscopy, pH therapy, Scanning Electron Microscope- Energy Dispersive X-ray (SEM-EDX).

1. Introduction

Nanotechnology has considerable promise for the detection, staging and treatment of cancer [1]. The past two decades have witnessed rapid advances in the ability to structure matter at the nanoscale with sufficient degree of control over the material size, shape, composition, and morphology [2]. The combination of the unique properties with the appropriate size has motivated the introduction of nanostructure into biology [3, 6] Cells and their constituent organelles lie on the sub-micron to micron size scale. Further, proteins and macromolecules found throughout the cell are on the nanometer size scale [7]. Thus nanoparticles ranging from a few to a hundred nanometers in size become ideal as labels and probes for incorporation into biological systems [5,6]

Despite significant investment and research, cancer is still responsible for 25% of all deaths in developed countries [8]. There is a pressing need for more sensitive, selective and cost-effective methods for detecting and treating cancer.

The presence of natural occurring nanoparticles that can produce apoptosis in cancer cells would be of great help. PMF, the active fraction separated from PM 701 [(natural product previously proved to be selective anticancer agent) [9-15] would give a promising therapeutic criterion in treating cancer. The effect of PMF on lung cancer cells A549

will be monitored by Fourier-transform infrared (FTIR) spectroscopy.

FTIR spectroscopy has become a useful analytical tool in biomedical science in the past decade, e.g., for the characterization of microorganisms[16], isolated cells or cell lines[17-20], body fluids and tissues [21,26] The ability to detect drug action, disease or dysfunction rapidly has obvious benefits, including early intervention of therapeutic strategies, hopefully in a prognostic fashion, significant reduction in mortality and morbidity, and the freeing up of much needed economic resources within health care systems [27]. With these highly sensitive techniques, the frequency and the intensity of light in the resulting spectrum provide biochemical information regarding the molecular composition, structure and interaction in cells and tissues.

Apoptosis, as a pre-programmed physiological mode of cell death, plays an important role in the pathogenesis and progression of cancer. Understanding of the basic mechanisms that underlie apoptosis will point to potentially new targets of therapeutic treatment of diseases that show an imbalance between cell proliferation and cell loss. As an active process, apoptosis involves biochemical changes on three essential cellular components, DNA, protein and lipid. There are three steps in apoptosis, the initiation phase triggered by a stimulus

received by the cell, the decision phase during which the cell commits itself to live or to die, and the degradation phase when the cells acquire the morphological and biochemical hallmarks of apoptosis [28]. Clearly, it would be desirable to detect apoptosis at an early stage, i.e. before phase that entails the visible changes of apoptosis.

In this study we will explore the potential of PMF as a selective anticancer agent which produces apoptosis in lung cancer cells (A549) by using FTIR spectroscopy technique and to bring to light the role of Cesium (Cs) and Rubidium (Rb) nanoparticles - found in PMF.

2- Material and Methods

Media

The following commercially available media were prepared according to published literature, these include: Ordinary media, Minimal essential medium (MEM, supplemented with 10%FCS): MEM is a rich, multipurpose medium that was used for cultivation of human lung cancer cells (A549). Phosphate Buffer Saline (PBS) is a Phosphate-Buffered physiological Saline solution. Calcium and Magnesium free Solution Trypsin [29] Examined media: PMF (extracted from PM 701) is a natural product, easily available, cheap, sterile, and non-toxic according to our chemical and microbiological testing. PMF added to the ordinary media with ratio 2.5 μg : 1 ml (w/v) media.

Human Lung Cancer Cells line:

Human Lung Cancer Cells, non- small cell carcinoma (A549) was obtained from cell strain from (ATCC) American Type Cultural Collection, available in the cell bank of Tissue Culture Unit, King Fahd Medical Research Center (KAU, Jeddah).

In vitro proliferation of cells

Human Lung Cancer Cells (A549) were suspended in culture medium MEM.

The cells were dispensed in 3X (6wells plate), 1×10^5 /ml in each well.

Each group of cells was incubated 24 hrs in suitable media and apoptosis was induced by incubating cells in PMF at different time points.

Infrared spectroscopy

At various time points, the cells treated with PMF were harvested and washed twice (by centrifugation for 3 min at 300 g). The cell pellet was kept at -80°C and freeze dried prior to IR measurements. The lyophilized samples - from three different separated experiments - were dispersed in potassium bromide (KBr) discs by mixing them gently in an agate mortar and with pestle to obtain

homogenous mixture as described previously [14, 30]. The mixture then pressed in a die at 5 metric tons force for 3 s, creating a 1.1 cm diameter transparent disc with imbedded sample. The FTIR spectra were recorded in absorbance form using Shimadzu FTIR-8400 s spectrophotometer with continuous nitrogen purge. The spectra were obtained in the wavenumber range of $4000-400\text{ cm}^{-1}$ with an average of 20 scans to increase the signal to noise ratio and at spectral resolution of 4 cm^{-1} . All the samples were baseline corrected and normalized to amide II band by using IR Solution software. The parameters studied were nucleic acid, proteins and lipids. Second derivative and difference method measurements were taken in comparison studies.

Scanning Electron Microscopy (SEM)

Detecting of Cs and Rb nanoparticles in PMF:

For SEM studies the PMF were suspended in distilled water, then treated in an ultrasonic bath (BRANSON, 1510) about 20 min. A small drop of this suspension placed on the double side carbon tape on Al- Stub and dried in air. The specimens were analyzed - without gold coating- by using energy dispersive analyzer unit (EX-23000BU) which attached to the scanning electron microscope (JSM-6360LA, JEOL, Tokyo, Japan). The microscope was operated at an accelerating voltage of 20 kV. Quantitative method ZAF and characterization method as pure.

Cs and Rb level measurements

Cs and Rb levels were measured in The Ministry of Petroleum-The Egyptian Mineral Resources Authority- Central Laboratories Sector by using Inductively Coupled Plasma (ICP) the results were multiplied by the dilution factor 20.1.

DNA fragmentation and pH measurements

DNA was extracted according to the method described by Kneipp et al., [23] by electrophoresis in agarose gel. The genomic DNA was run in a 1.5% agarose gel for 20min.

The pH values of the A549 cell's media were measured immediately by Jenway 3200 pH meter at the end of each treating time. These measurements were repeated for three different experiments.

3. Results and Discussion

IR spectral features and assignments

The addition of PMF to A549 cells after 5, 15, 30 min and 2, 24hr of treatment caused a series of changes in the spectra of these cell lines (Fig.1). The absorption profiles are typical of tissue infrared spectra, which are dominated by protein, lipids and DNA represents the most absorption IR spectral

peaks and the proposed biomolecular assignments (Table I). Fig.1a. shows a noticeable decrease in the intensities of proteins (amide I & amide II), nucleic acids band, and an increase in the intensity of the weak shoulder located at 1737 cm⁻¹ after PMF treatment.

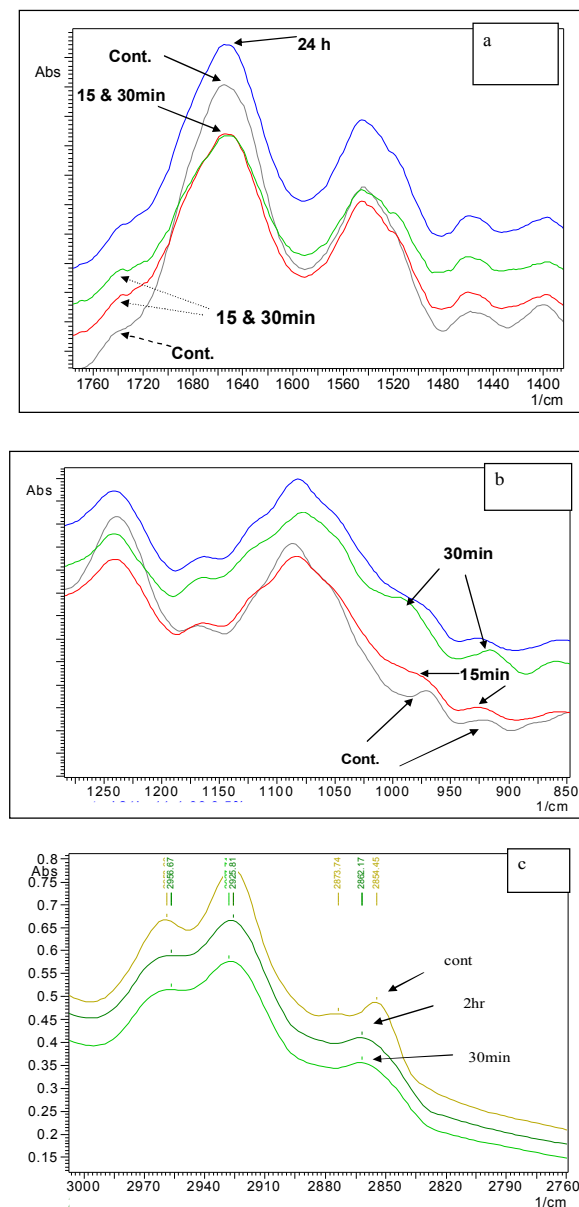


Fig. 1 Raw FTIR spectra of A549 cells treated with PMF at different times (a) shows the amide I band shift and the increase in the intensity of the band located at 1735 cm⁻¹ (C=O ester group) in range 1760-1400 cm⁻¹. (b) shows the decrease in DNA peaks at the onset of apoptosis (5-15min) and the increase in 970 cm⁻¹ peak after 30 min of PMF treatment. (c) shows the band shift in CH₂ bands.

TABLE 1. Major IR Spectral Peaks Of A549 Cells and Proposed Biomolecular Assignments

Wave number (cm ⁻¹)	Proposed biomolecular assignment
2963	C-H stretch (asymmetric) of CH ₃ in fatty acids, lipids, proteins.
2926	C-H stretch (asymmetric) of CH ₂ in fatty acids, lipids, proteins.
2873	C-H stretch (symmetric) of CH ₃ in fatty acids, lipids, proteins.
2853	C-H stretch (symmetric) of CH ₂ in fatty acids, lipids, proteins.
1737	Ester C=O stretching of phospholipids.
1652	Amide I of α -helix protein structures (C=O) stretch.
1542	Amide II (N-H) bend
1460	CH ₃ antisymmetric bend
1430-1360	COO ⁻ stretch
1240	PO ₂ ⁻ asymmetric stretch of phosphodiester group in nucleic acids and phospholipids
1168	C-O, C-C stretch, C-O-H, C-O-C deformation of carbohydrates or C-OH stretch of serine, threonine, tyrosine in cell proteins
1085	PO ₂ ⁻ symmetric stretch of phosphodiester group in nucleic acids and phospholipids
975	PO ₃ ²⁻ stretch

We also observed that the amide I band shifted towards lower frequency from 1652 cm⁻¹ in the control cells to 1649 cm⁻¹ in the cells treated with PMF for 15, 30 min, 2hr and 24hrs. These amide I frequencies are compatible with the fact that overall protein structure in the control cells consists primarily of α -helix, whereas after 5min up to 24hr of PMF treatment the cells have a relatively high proportion of β -sheet and a relatively high proportion of unordered proteins. A similar shift in the amide I and amide II bands during apoptosis was reported earlier [14,35,39].

Alterations in lipid content/structure can also be obtained by examining the dominant lipid bands in the range 2800-3050 cm⁻¹ that originate from CH stretching vibrations of the fatty acyl chains of all cellular lipids (Fig.1b). The CH₂ band provide information about the membrane fluidity [40], the higher the frequency, the higher the fluidity. Therefore, we analyzed the CH₂ band position in the cells before and after PMF treatment and found that for control A549 cells this band was centered at 2931 cm⁻¹ while it is shifted to 2929 cm⁻¹ in the treated cells. This observed shift in CH₂ band could be explained. It can be considered now as a strong evidence in decreasing membrane fluidity, which would be in agreement with oxidative damage having occurred [36, 39].

Absorbance of infrared in the region 900-1300cm⁻¹ of the samples is shown in Fig.1c. The figure shows the decrease in DNA peaks at the onset

of apoptosis (5-15min) and the increase in 970 cm^{-1} peak after 30 min of PMF treatment. Early apoptotic cells appear in the cell cycle distribution as cells with a hypodiploid DNA. This alteration in DNA content results from degradation of cellular DNA by activation of endogenous endonucleases during apoptosis [36]. Cells in the pre-Go/G1 phase (M4) were therefore defined as apoptotic cells. These results are also consistent with the finding that at the early stage of apoptosis, initiation phase is triggered by a stimulus received by the cell, this can be explained by the first disappearance of nucleic acid bands at 975 and 923 cm^{-1} at 5 and 15 min upon PMF treatment. A549 cells treated up to 30 min with PMF showed clear absorbance bands of DNA at 975 and 923 cm^{-1} which may referred to the degradation of DNA. Jamin et al. [41] reported a large increase in the DNA signals of apoptotic cells. In apoptosis DNA is degraded into oligonucleotides with a few hundreds of base pairs that subsequently diffuse out of the nucleus. This observation suggests that the DNA, although highly condensed in the nucleus, has a low absorption, yet its degradation products in late apoptosis are detected by IR spectroscopy.

Fig. 2 represents the raw IR spectra of A549 cells treated with PMF from 5 min up to 24hr without normalization. The figure shows a dramatic decrease in bands intensities over the rang 1800-900 cm^{-1} . The same results were obtained from normal human fetal lung fibroblast IMR-90 in G1, S-, and G2M-phase of the cycle [39]. Hoi-Ying et al., [39] showed that the IR spectra of these three phases are clearly different. During the S-phase the DNA was undergoing replication and they observed that the absorption in the DNA/RNA spectral region increased relative to the G1-phase spectra. When a G2/M-phase cell was measured they observed a large increase in the overall absorbance ([like the uppermost spectrum in Fig. 2. This may have been a result of more material in the cell or because of the thickness may have been different in the M-phase.

Second Derivative Analysis

Since apoptosis involves the modification of existing proteins, as well as the synthesis of new proteins [35, 39] we analyzed the changes of protein structure after PMF treatment in more detail. Fig. 3 shows only the mean spectra of control and PMF treated cells for 30 sec - for clarity reason - in the region of the amide I (1600-1700 cm^{-1}) and amide II (1500-1600 cm^{-1}) bands. Spectra are shown as second derivative, a method commonly used for narrowing broad IR bands for better visualization. The spectrum of a dying cell due to treatment shows significant shifts in the amide I peak compared to the spectrum of a living A549 cell. The changes in the secondary

structure of the proteins appeared after 15 min of treatment. The dying cell shows two characteristic spectral signatures indicative of death [36, 41]. First, the centroids of the protein amide I and II peaks shift to lower energy, indicating a change in the overall protein conformational states within the cell. Second; the appearance of a peak at around 1743 cm^{-1} [39]. These structural changes in the cellular proteins could be due to a different distribution of proteins during apoptosis or to denaturation of the existing proteins.

The lipids in the plasma membrane are composed mainly of phospholipids that determine membrane stability, fluidity and membrane enzymatic activity [40]. Thus, monitoring lipid absorbance in the treated samples is an important for detecting apoptosis. The peak at 1737 cm^{-1} - which is associated with the non-hydrogen bonded ester carbonyl C=O - splits into two bands in the second derivative analysis (Fig 3.) centered at 1743 and 1725 cm^{-1} . the reason that the 1743 cm^{-1} peak in Fig.3 is significantly more intense than the 1725 cm^{-1} peak implies that the C=O ester carbonyl groups of lipids in the cell are becoming predominantly non-hydrogen bonded, which would be in agreement with oxidative damage having occurred [39]. Apoptosis is associated with, among other factors, increased oxidative damage [42, 43]. The positive intensity at 1740 cm^{-1} suggest an increase in the C=O ester components in the plasma membranes following PMF treatment.

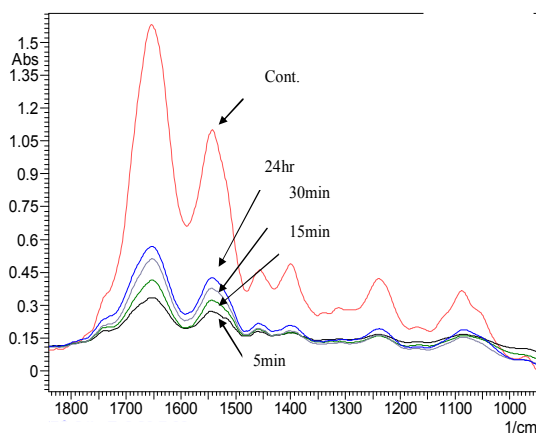


Fig. 2 The raw FTIR spectra of A549 cells treated with different times with PMF. The spectra were not normalized.

Difference Method

In order to further assess and identify these membrane changes, typical IR marker bands for lipids were evaluated by creating a difference spectrum' in the range of 2800-3050 cm^{-1} Fig. 4(a).

The two methyl bands at 2870 and 2954 cm^{-1} , which originate from the symmetric and asymmetric stretching vibrations of the acyl chain CH_3 groups,

are negative in the IR 'difference spectrum' in contrast, the two methylene bands at 2851 and 2931cm^{-1} , attributed to the symmetric and asymmetric stretching vibrations of acyl chain CH_2 groups are positive, indicating that PMF treatment increases the lipid content in the plasma membranes of A549 cells.

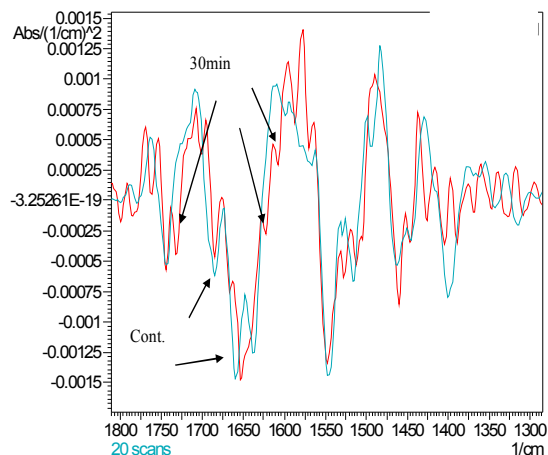


Fig. 3 Infrared second derivative spectra of control and PMF-treated A549 cells for 30 min.

The characteristic CH_3 group stretching vibration bands at 2870 & 2954cm^{-1} show a negative band in the difference spectrum. These results may reflect structural changes of phospholipids rather than relative changes of lipid in the treated cells [34, 35]. PMF contains mainly peptides and amino acids [44]. Thus, PMF may contact with A549 cell membrane and may form some sort of an ion channel or pore in the cell membrane thereby, enhancing the ion permeability of the membrane and destroying the cell i.e. induce apoptosis. References [45-47] suggested that the peptide could perturb membrane functions responsible for osmotic balance.

The mode of action of PMF with the membrane phospholipids bilayers could possibly be due to the aggregation of peptides on the surface of the membrane and then inserts into the bilayer forming a so-called barrel-stave pore. Another possibility is that the accumulation of peptide on the membrane surface forms a destabilizing carpet, leading to a local disintegration of the bilayer. A third possibility is that peptide chains aggregate on the membrane surface, possibly forming a carpet, partially submerge, and then blend with lipids so that peptide chains and lipid head groups together line the wall of a toroidal pore [35, 44-48].

The present and our previous study [14] extend these findings and suggest that PMF may alter the conformation of membrane proteins such as

nucleoside transporters, ion channels and proof the formation of pores.

The Transmission Electron microscope (TEM) Photograph (Fig. 5) was taken after 5 sec only from adding PMF to the media "unpublished paper" [49]. The arrow in the Fig. pointed to the entrance of nanoparticles to inside the nucleus via temporary created artificial pore (T) in the nuclear envelope. The nanoparticle interpenetrated the nuclear envelope and the underneath euchromatin. The normal nuclear pore was also seen in other place, whereas no underneath chromatin prevent the normally entrance and exit of molecules.

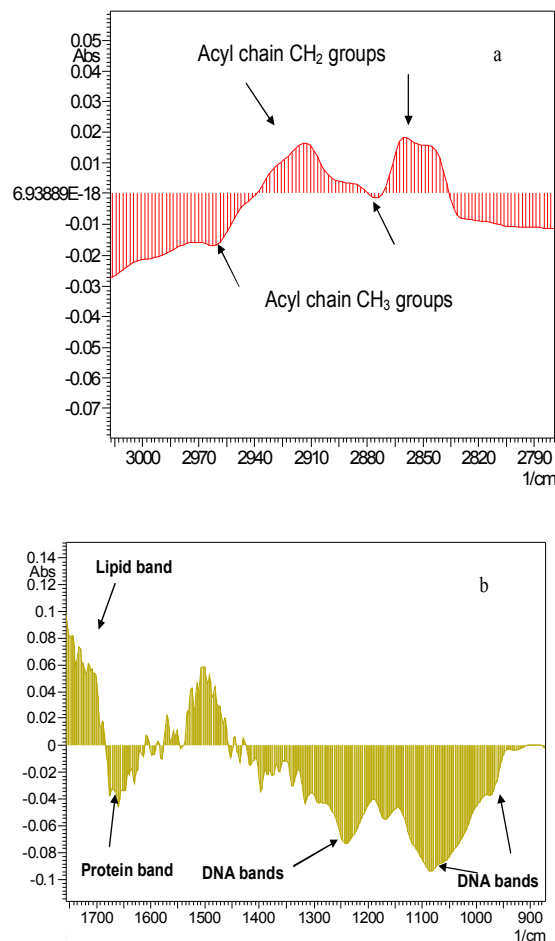


Fig. 4 The IR difference spectrum between control and PMF treated A549 cells for two hours in range 3000 - 2800cm^{-1} (a). Difference spectra between control A549 cells and that treated with PMF for 5 min. The figure shows negative DNA bands (at 930cm^{-1} , 1085cm^{-1} and 1240cm^{-1}), negative band of proteins (1652cm^{-1}) and positive band of lipids (1735cm^{-1}) (b).

Difference spectra between control A549 cells and that treated with PMF for 5 min in range 1700 - 900cm^{-1} were presented in Fig. 4b. The figure

shows negative DNA bands (at 930cm^{-1} , 1085cm^{-1} and 1240cm^{-1}), negative band of proteins (1652cm^{-1}) and positive band of lipids (1735cm^{-1}). From the difference spectrum one can clearly observe that DNA content in the cells treated with PMF has significantly decreased. These results are consistent with the finding that condensation of chromatin during the early stage of apoptosis takes place which in turn decreases the path length [41,50]. This is may referred to dark DNA, one would expect that less photons are transmitted within the strong absorption bands of DNA (which make up the chromatin) by particles of such relatively high optical density. Furthermore, given the entire highly condensed chromatin would be virtually opaque [41, 50]. These results are in good agreement with the results obtained earlier [10,14] who studied the effect of PM701 as anticancer agent in vitro on the same type of cancer A549 cells. Live images of the cells showed that the severe lethal effects of PM701 on cancer cells started immediately after 5-6min since adding the examined substrate. They continued that the cancer cells incubated in PM701 showed that the substrate attacks the cell's nuclei, which is indicated by the appearance of pale ring around the nucleus of the lung cancer cell after 30 min of incubation. This leads to the degradation of the cells, which could not be reversed to recover the cells by re-growing the cells in ordinary media again.

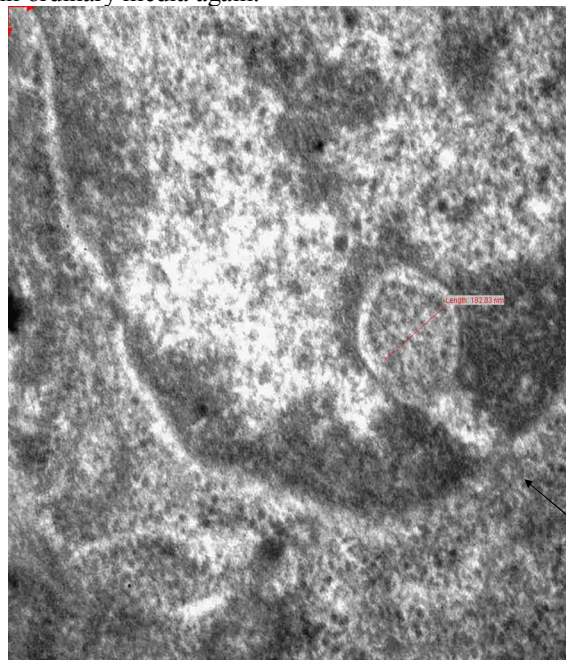


Fig. 5 TEM image of A549 cells after 5 sec of PMF treatment. The figure shows the induced pore formation in the nucleus membrane upon PMF treatment.

Electrophoresis and pH measurements

We extracted DNA from A549 control and the treated cells to confirm the finding that PMF induces apoptosis and analyzed DNA fragmentations using gel electrophoresis. A characteristic internucleosomal ladder of DNA fragmentation was observed in A549 cells treated with PMF for 30 min (Fig. 6). These results are in good consistent with the above results obtained from infrared spectroscopy observations.

The pH values of the A549 cells were measured as described earlier. The relationship between the time of treatment and the pH values were shown in Fig. 7. For all times of treatment, the pH values increased significantly after adding PMF to the media of A549 cells the maximum value was obtained at 2hrs of treatment. Our results consistent with the previous reported results describing the pH value of cancer cells and the using of high pH therapy in cancer patients [48, 51, 52]. The cancer cells contain high amounts of hydrogen ions rendering them acidic and they also contain higher Na^+ levels than found in normal cells. If Cs^- or Rb^- enters the cancer cells, their pH increases. At a pH of 7.6 the cancer cell division will stop, and at a pH of 8.0 to 8.5 the life span of cancer cells is considerably shortened to only hours [51]. Cs, Rb, and the other elements were detected in PMF by using SEM-EDX (Fig. 8) (Table II). The presence of Cs or Rb in the fluids adjacent to the tumor cells is believed to raise the pH of the cancer cells where cell mitoses will then cease resulting in reduction of life span of the cancer cell [52].

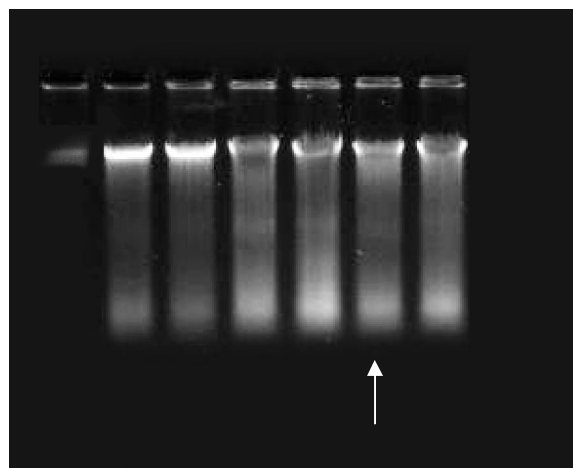


Fig. 6 Detection of DNA fragmentation by agarose electrophoresis. A549 cells were treated with PMF for 5, 15, 30 min, 2hr and 24hr with PMF (Lane from left to right). The arrow points to DNA maximum fragmentation after 30 min of treatment.

(Ag) and gold (Au) nanoparticles [49]. Noble metal, especially Au, nanoparticles have immense potential for cancer diagnosis and therapy [7].

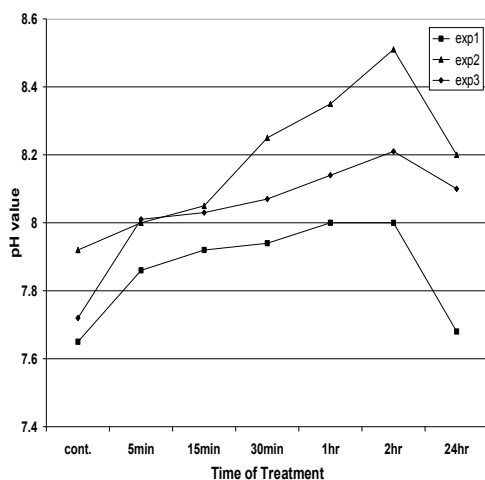


Fig. 7 The pH values of three different measurements to the A549 cells' media for different PMF treating time. The results obtained from three different separated experiments.

The mechanism of action of Cs in cancer has been little studied. That both Cs⁻ and Rb⁻ can specifically enter cancer cells and embryonic cells, but not normal adult cells[51]. PMF contain 70.9128, 8.04 ppm Rb and Cs respectively and thus may explain the selectivity action of this new anticancer agent (PMF). It is clear from (Table II) that PMF contain also silver

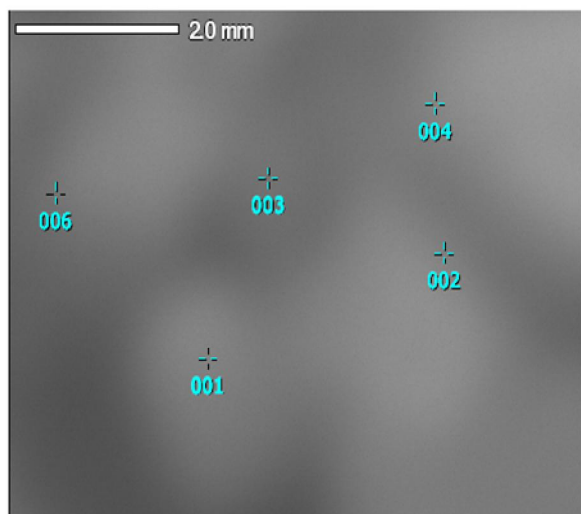


Fig. 8 SEM-EDX image of PMF

TABLE II The most important nanoparticles detected in PMF by SEM-EDX

mass%	N	Na	Mg	P	S	Cl	K	Ca	Cu	Zn	Rb	Ag	Cs	Au	Total
001	55.45	14.04	2.32		1.02	15.96	8.74	1.07	0.10	0.07	0.23	0.88			1.33
002	47.36	21.07	1.74	0.20	0.96	21.18	7.28	0.30		0.22	0.28				100.00
003	52.78	17.77	1.65		0.93	17.87	8.38	0.26	0.05			0.15		0.78	100.00
004	52.58	16.34	0.82		0.22	17.94	9.76	0.21		0.14	0.95	0.52	0.23		100.00
006	53.23	17.78	1.42		0.75	17.64	8.84	0.54	0.03	0.28	0.43	0.63	0.42		100.00

Conclusion

To conclude, we can state that PMF can induce apoptosis to A549 cells. The dominant protein secondary structure shifts from α -helix structure to unordered, indicating an altered protein profile in the apoptotic cells. In addition the total cellular lipid content increases starting from the first 5 to 15 min up to 24hr of treatment while the amount of DNA decreases dramatically during treatment with PMF as observed in difference spectrum

It should mention here that condensation of chromatin at the early stage of apoptosis was observed after 5 to 15 min of PMF treatment in the FTIR spectra indicated by the disappearance of the DNA absorbance bands. On the other hand, fragmentation of chromatin after 30 min of PMF treatment was evident by both FTIR spectroscopy and formation of DNA Ladder in the electrophoresis analysis. This study indicates that PMF contains Cs and Rb nanoparticles which proved to have a role in attacking cancer cells by elevating the pH. Thus, PMF as a natural product gives promising hope in cancer therapy with its prosperity of different potentially variable nanoparticles. These nanoparticles nowadays are all represent the new trend in treating cancer.

Corresponding author

Nahla AG Ahmed Refat

Department of Pathology, Faculty of Veterinary Medicine, Zagazig University, Egypt

Nahla_kashmery@hotmail.com

References

- [1] Paolo F., J. K. Larry, J. G. David, P. Jason, H. Terry, T. Felicia, H. Naomi, S. Saul, A. W. Scott, 2007. "Applications of nanoparticles to diagnostics and therapeutics in colorectal cancer," *TREND Biotechnology*, 25, : 145-152
- [2] Burda C., X. Chen, R. Narayanan, and M. A. El-Sayed, 2005. "Chemistry and properties of nanocrystals of different shapes," *Chem. Rev.*, 105: 1025-1102.
- [3] Katz E., I. Willner, 2004. "Integrated Nanoparticle-Biomolecule Hybrid Systems: Synthesis, Properties, and Applications," *Angew. Chem. Int. Ed. Vol.*, 43: 6042.

- [4] Rosi N. L., C. A. Mirkin, 2005. "Nanostructures in Biodiagnostics," *Chem Rev.*, 105: 1547.
- [5] Salata O. V., 2003. Applications of nanoparticles in biology and medicine, *J. Nanobiotech.* 2:3.
- [6] Whitesides G. M., 2003 "The 'right' size in nanobiotechnology," *Nat. Biotech.*, 21:1161.
- [7] Prashant K. J., H. Ivan, M. A. El-Sayed, 2007. "Au nanoparticles target cancer.," *Nanotoday*, 2: 18-29.
- [8] **Jemal A.**, T. Murray, E. Ward, A. Samuels, R. C. Tiwari, A. Ghafoor, E. J. Feuer, and M. J. Thun, 2005. Cancer Statistics, *CA. Cancer J. Clin.*, 55:, pp. (4):259.
- [9] Khorshid F. A., S. S. Moshref, N. Heffny, , 2005. An ideal selective anticancer agent in vitro, I-Tissue culture study of human lung cancer cells A549," *JKAU- Medical Sciences*, 12: 3-18.
- [10] Moshref S. S., F. A. Khorshid, Y. Jamal, 2006. The effect of PM 701 on mice leukemic Cells: I - Tissue culture study of L1210 (in vitro) II - In vivo study on mice," *JKAU- Medical Sciences*. 13:3-19. vol 13 (1), pp. 3-19.
- [11] Khorshid F. A., S. S. Moshref ,2006 "In vitro anticancer agent, I - Tissue culture study of human lung cancer cells A549 II - Tissue culture study of mice leukemia cells L1210," *International Journal of Cancer Research*, vol., 2, no. 4, pp. 330-344.
- [12] Moshref S. S., 2007 "PM701 a highly selective anti cancerous agent against L1210 leukemic cells: II – In vivo clinical and histopathological study," *JKAU- Medical Sciences*, vol., 14, no. 1, pp. 85-99, 2007.
- [13] Khorshid F.A., 2009 "Potential anticancer natural product against human lung cancer cells," *Trends Med. Res.*, vol., 4, no. 1, pp. 9-15.
- [14] Raouf G. A. , F. A. Khorshid , T. Kumosani, 2009 "FT-IR Spectroscopy as a Tool for Identification of Apoptosis-Induced Structural Changes in A549 Cells Dry Samples Treated with PM 701," *Int.J. Nano and Biomaterials*, vol., 2, no. 1/2/3/4/5, pp. 396-408.
- [15] Khorshid F. A., A. M. Osman, E. Abdel-Sattar, 2009 "Cytotoxic activity of bioactive fractions from PM 701," *EJEAFChe*, vol., 8, no. 11, pp. 1091-1098.
- [16] Naumann D, D. Helm, Labischinski, 1991 "Microbiological characterization by FT-IR spectroscopy," *Nature*, vol., 351, pp. 81-2.
- [17] Diem M., S. Boydston-White, & L. Chiriboga, 1999 "Infrared spectroscopy of cells and tissues: shining light on a novel subject," *Appl. Spectrosc.*, vol., 53, 148A-161A ,.
- [18] Fabian H., D. Chapman, H. Mantsch, 1996 "Infrared Spectroscopy of Biomolecules," Mantsch, H. H., Chapman, D., Eds., *Wiley-Liss*: New York, pp 341-352.
- [19] Schulz, C. P., L. Kan-Zhi, B. J. James, H. M. Henry, 1997 "Prognosis of chronic lymphocytic leukemia from infrared spectra of lymphocytes," *J. Mol. Struc.*, vol., 408, no. 40, pp. 253-256.
- [20] Baker M. J., E Gazi, M.D. Brown, J.H. Shanks, P. Gardner, N.W. Clarke, 2008 "FTIR-based spectroscopic analysis in the identification of clinically aggressive prostate cancer," *British J. Cancer*, vol., 99, pp. 1859-1866.
- [21] Lasch P., D. Naumann, 1998 "FT-IR microspectroscopic imaging of human carcinoma thin sections based on pattern recognition techniques," *Cell. Mol. Biol.* vol., 44, no. 1, pp. 189-202.
- [22] McIntosh L., M. Jackson, H. Mantsch, M. Stranc, D. Pilavdzic, A. Crowson, 1999 "Infrared spectra of basal cell carcinomas are distinct from non-tumor-bearing skin components," *J. Invest. Dermat.*, vol., 112, pp. 951-956.
- [23] Kneipp J., P. Lasch, E. Baldauf, M. Beekes, D. Naumann, 2000 "Detection of pathological molecular alterations in scrapie-infected hamster brain by fourier transform infrared (FT-IR) spectroscopy" *Biophys. Acta.*, vol., 1501, no. 2-3, pp. 189-99.
- [24] Roeges N. P., 1994 "A Guide to complete interpretation of Infrared Spectra of Organic Structures," *Wiley*, Chichester, UK.
- [25] Mantsch H. H., D. Chapman, 1996 "Infrared Spectroscopy of Biomolecules" *Wiley-Liss*, New York.
- [26] Brandenburg K., U. Seydel, 1998 "Infrared Spectroscopy of Glycolipids," *Chem. Phys. Lipids*, vol., 96, pp. 23.
- [27] David I., G. Royston, 2006 "Metabolic fingerprinting in disease diagnosis: biomedical applications of infrared and Raman spectroscopy," *Analyst*, vol., 131, pp. 875-885.
- [28] Huilu Y., T. Zhanhua, A. Min, P. Lixin, W. Guiwen, H. Bijuan, L. Yong-qing, 2009 "Raman spectroscopic analysis of apoptosis of single human gastric cancer cells" *Vibrational Spectroscopy*," *Vib. Spectrosc.* vol.50, pp.193-197.
- [29] Giaever I., C. R. Keese, 1986 *IEEE Transactions on Biomedical Engineering BME-33* (2), pp. 242-247.
- [30] Paul G. L., D. S. Robert, 1998 "Cancer grading by Fourier transform infrared spectroscopy," vol., 4, pp. 37-46.
- [31] Montpetit S. A., I. T. Fitch, P. T. O'Donnell, 2005 "A simple automated instrument for DNA extraction in forensic casework," *J. Forensic Sci.*, vol., 3, no. 555-63.

- [32] Jackson M., M.G. Sowa, H. H. Mantsch, 1997 "Infrared spectroscopy: a new frontier in medicine," *Biophys. Chem.*, vol. 68, 109-125.
- [33] Wong P. T., R. K. Wong, T.A. Caputo, T. A. Godwin, B. Rigas, 1991 "Infrared spectroscopy of exfoliated human cervical cells: evidence of extensive structural changes during carcinogenesis," *Proc. Natl Acad. Sci., USA* vol., 88, pp. 10988-10992,.
- [34] Mantsh H. H., 2001 "Apoptosis-induced structural changes in leukemia cells identified by IR spectroscopy," *J. Mol. Str.*, vol., 565-566, pp. 299-304,.
- [35] Liu K-Z, Li Jia., S. M. Kelsey, A. C. Newland, H. H. 2001 "Mantsch, Quantitative determination of apoptosis on leukemia cells by infrared spectroscopy," *Apoptosis*, vol., 6, pp. 269-278.
- [36] Rigas B., & P. T. Wong, 1992 "Human colon adenocarcinoma cell lines display infrared spectroscopic features of malignant colon tissues," *Cancer Res.*, vol., 52, pp. 84-88.
- [37] Benedetti E., E. Bramanti, F. Papineschi, & I. Rossi, 1999 "Determination of the relative amount of nucleic acid of the relative amount of nucleic acids in leukemic and normal lymphocytes by means of FT-IR microscopy" *Appl. Spectrosc.*, vol., 51, pp. 792-797,.
- [38] Boydston-White S., T. Gopen, S. Houser, J. Bargonetti, & M. Diem, 1999 "Infrared spectroscopy of human tissue. V. Infrared spectroscopic studies of myeloid leukemia (ML-1) cells at different phases of the cell cycle" *Biospectroscopy*, vol., 5, pp. 219-227.
- [39] Hoi-Ying N. H., C. M. Michael, A. B. Eleanor, B. Kathy, R. M. Wayne, 2000 "IR spectroscopic characteristics of cell cycle and cell death probed by synchrotron radiation based Fourier transform IR spectroscopy," *Biopoly. Biospectrosc.*, vol., 57, pp. 329-335,.
- [40] Casal H. L., H. H. Mantsch, Polymorphic phase behaviour of phospholipid membranes studied by infrared spectroscopy. *Biochem. Biophys. Acta* 779 (1984) 381-401.
- [41] Jamin N., L. Miller, J. M. Fridman, W. H. Dumas and J. L. Teillaud, 2003 "Chemical heterogeneity in cell death: combined synchrotron IR and fluorescence microscopy studies of single apoptotic and necrotic cells," *Biopoly. Biospectrosc.*, vol., 72, pp. 366-373,.
- [42] Mittler R, 1998 "In when cells die: A comprehensive evaluation of apoptosis and programmed cell death," Lockshin,R., Zakeri Z., Tilly J., Eds.; *Wiley-Liss*: New York, pp.147-174,.
- [43] Birge R., E. Fajardo, B. Hempstead, 1998 "In when cells die: A comprehensive evaluation of apoptosis and programmed cell death," Lockshin,R., Zakeri Z., Tilly J., Eds.; *Wiley-Liss*: New York, pp. 347-384,.
- [44] El-Shahawy A., N. M. Elswawi, W. S. Baker, F. A. Khorshid, N. S. Geweely, 2010 "Spectral analysis, molecular orbital calculations and antimicrobial activity of PMF- G fraction extracted from PM-701" *Int. J. Pharm. Bio. Sci.*, vol., 1, no. 2.
- [45] Matsuzaki K., "Magainins as paradigm for the mode of action of pore forming polypeptides" *Biochem. Biophys. Acta.*, vol., 1376, pp. 391-400, 1998b.
- [46] Shai Y., 1999 "Mechanisms of the binding, insertion and destabilization of phospholipids bilayer membrane by α -helical antimicrobial and cell nonselective membrane-lytic peptides" *Biochem. Biophys. Acta*, vol., 1462, pp. 55-70.
- [47] Zasloff M., 1987 "Magainins, a class of antimicrobial peptides from *Xenopus* skin: Isolation, characterization of two active forms, and partial c DNA sequence of a precursor" *Proc. Natl., Acad. Sci. USA*, vol., 84, pp. 5449-5453.
- [48] Matsuzaki K., O. Murase, N. Fujii, K. Miyajima, 1995 "Translocation of a channel-forming antimicrobial peptide, magainin 2, across lipid bilayers by forming a pore" *Biochemistry*, vol., 34, pp. 6521-6526,.
- [49] Raouf G. A. , F. A. Khorshid, S. M. El-Hamidy, G. S. Al-amri, N. A. Alotaibi, T. Dakhakhni, "PMF nano-shells and Quantum dots for cancer therapy," unpublished paper.
- [50] Brian M., R. Melissa, D. Max, and R. W. Bayden, 2005 "Mie-Type Scattering and non-Beer-Lambert Absorption Behavior of Human Cells in infrared Microspectroscopy, " *Biophysical J.*, vol., 88, pp. 3635-3640.
- [51] Brewer K.A., 1979 "Mechanism of carcinogenesis: Comments on therapy" *J. Int. Acad. Prev. Med.* , vol., 5, pp. 29-53,.
- [52] Sartori H. E., 1984 "Cesium therapy in cancer patients," *Pharm. Biochem. & Behavior*, vol., 21, pp. 11-13.